Dynamics of Copolymer Micelles in an Entangled Homopolymer Matrix

Kerstin Gohr,[†] Tadeusz Pakula,[‡] Kiyoharu Tsutsumi,[§] and Wolfgang Schärtl*[,†]

Institut für Pysikalische Chemie, Universität Mainz, Welderweg 11, 55099 Mainz, Germany, Max-Planck Institut für Polymerforschung, Ackermannweg 10, 55021 Mainz, Germany, and Hashimoto Polymer Phasing Project, ERATO, JRDC, Japan, 15 Morimoto-Chyo, Shimogamo Sakyoku, Kyoto 606, Japan

Received April 12, 1999; Revised Manuscript Received July 19, 1999

ABSTRACT: The dynamics of block copolymer micelles, with a glassy polystyrene core and polyisoprene corona, in a matrix of linear entangled polyisoprene (PI) chains, has been investigated by forced Rayleigh scattering (FRS), dynamic mechanical measurements, and dielectric relaxation spectroscopy. The concentration of micelles has been varied from 10 to 50 wt % copolymer. FRS measurements revealed two dynamical processes at low temperature. The slower of these processes has been identified as micellar diffusion, the faster as rotation of individual micelles. Dynamic mechanical measurements have shown three relaxation modes: (i) PI segmental relaxation; (ii) relaxation of matrix chains or of corona polyisoprene blocks; (iii) relaxation of individual micelles. The first two processes have been confirmed by dielectric relaxation spectroscopy, whereas the slowest one has coincided with the relaxation time related to self-diffusion of micelles detected by FRS when extrapolated to the length scale of the micelle dimensions. Results are also compared to those of recent studies of copolymer micelles in a nonentangling homopolymer matrix.

Introduction

Spherical block copolymer micelles of type AB (i.e., core A, corona B) embedded in a homopolymer melt of type B provide a very interesting model system. Dependent on microdomain concentration, they show a phase behavior very similar to that of hard sphere colloidal particles.[1] At high concentrations, small-angle X-ray scattering (SAXS) measurements indicate a cubic paracrystalline, i.e., distorted, structure,[2,3] whereas, at lower concentrations, the micelles are expected to show a liquid-like arrangement. Kinning and Thomas[4] have shown that the paracrystalline structure in many cases also may be analyzed by the Percus Yevick model of hard spheres. This seems to indicate a more liquid-like arrangement of micelles even at high concentrations. The strongly repulsive interactions between spherical block copolymer micelles, which control the phase behavior of the system, have been investigated theoretically by Leibler and Pincus.[5] They explained the repulsive interaction potential by an effective decrease of homopolymer chains in the outer shell of overlapping copolymer micelles, leading to an energetically unfavorable condition. Consequently, the molecular weight of the linear homopolymer matrix chains plays a significant role in interparticle interactions of the micelles. In the case of homopolymer chains of molecular weight smaller than that of the corona block of the micelle, the corona is strongly swollen by the homopolymer (wet brush conditions). Therefore, the repulsive effect is much stronger than in the case of a high molecular weight matrix homopolymer which only shows little swelling of the micellar corona (dry brush conditions). In addition to their colloidal-analogous phase behavior, spherical micelles also are a model for highly branched polymer systems (multiarm star polymers).[6−8]

For all these reasons, the experimental study of the dynamics of block copolymer micelles in a homopolymer melt provides a subject of major scientific interest. Watanabe and co-workers have published extensive rheological measurements of spherical block copolymer micelles with glassy polystyrene (PS) cores and polyisoprene (PI) or polybutadiene (PB) corona embedded in a matrix of linear PI or PB.[9−15] They studied the effects of micellar concentration as well as matrix molecular weight, the latter adjusting from nonentangling (M < 5000 g/mol) to highly-entangled dry brush (M > 100 000 g/mol) conditions. A nice review of these earlier experiments is given in a recent feature article by Watanabe.[16] Rheology of block copolymer micelles in a homopolymer melt revealed three relaxational processes. The fastest process is attributed to relaxation of the matrix homopolymer. The intermediate mode has been identified as relaxation of individual corona blocks, whereas the slowest process has tentatively been attributed to self-diffusion of block copolymer micelles. To obtain a quantitative measure of the diffusion time, Watanabe et al. have calculated an effective relaxation time for the slow process according to the Stokes−Einstein equation:

$$\tau_{SE} = \pi R \eta \delta^2 / kT \qquad (1)$$

Here, R is the radius of the micelles, η the effective viscosity for the micellar diffusion, and δ the diffusion distance. kT is the thermal energy which generates the Brownian motion of the particles. For dilute nonentangled micelles, the effective viscosity has been assumed as given by the viscosity of the matrix homopolymer. As diffusion distance, the particle diameter has been chosen, i.e., $\delta = 2R$. Opposite the findings for nonentangling homopolymer matrices, a surprising result has been obtained for entangling homopolymers: at low micellar concentrations, the relaxation time of the slow process found in rheological measurements is much smaller than τ_{SE} determined by eq 1.

* To whom correspondence should be addressed. E-mail: schaertl@mail.uni-mainz.de.
[†] Universität Mainz.
[‡] Max-Planck Institut für Polymerforschung.
[§] ERATO, JRDC.

10.1021/ma990549m CCC: $18.00
Published on Web 09/21/1999

These so far unexplained results from rheology emphasize the necessity of the experimental investigation of the self-diffusion itself of spherical block copolymer micelles.

The first self-diffusion studies of block copolymer micelles with a glassy PS core and PI corona in a PI homopolymer melt at very high concentrations have been carried out by forced Rayleigh scattering (FRS).[17] By now, these early studies have been extended from highly concentrated interentangling micellar systems to moderate concentrations of nonoverlapping micelles embedded in an entangling PI matrix.[18] Recently, the dynamics of PS−PI micelles in a nonentangling PI matrix as a function of micellar concentration in this moderate concentration regime has been studied by Watanabe et al.,[19] using both FRS and rheological measurements. The authors reported two relaxation processes for the FRS measurements. The slower process has been attributed to self-diffusion of spherical micelles. Correspondingly, the terminal relaxation process of the rheological studies has been identified as self-diffusion of spherical micelles over a distance of the micellar core diameter. No definite explanation has been given for the fast process.

In this paper, the investigation of the dynamics of block copolymer micelles in a long-chain interentangled homopolymer matrix over a wide concentration range from dilute to strongly interentangled, using a combination of various techniques such as FRS, dynamic mechanical spectroscopy, and dielectric spectroscopy, is reported. Results are also discussed with respect to the studies of similar block copolymer micelles in a short-chain nonentangled homopolymer matrix by Watanabe et al.[19] Here, the microstructure of the micelles, i.e., the swelling of the micellar corona, is expected to depend only on the molecular weight of the matrix homopolymer with respect to the corona block, whereas the entanglement character of the matrix chains should be insignificant.

Experimental Section

Materials. The asymmetric PS-*b*-PI diblock copolymer (SI) was synthesized by sequential living anionic polymerization in cyclohexane at 50 °C, using *sec*-butyllithium as initiator. Part of the living block copolymer was terminated with methanol, the other with an excess of α,α′-dichloro-*p*-xylene to introduce a functional chloromethyl group at the PS chain end of the diblock. The chloromethyl group is used to attach the photoreactive dye label *o*-nitrostilbene[20−22] onto the diblock copolymer. Such photoreactive labeling is necessary for diffusion studies by FRS.

It should be noted that the bifunctional termination reagent leads to a small amount (<30%) of binary coupling of diblock copolymers. This coupling decreases the labeling efficiency due to a decrease in chloromethyl functionalization. However, the presence of coupled block copolymer chains (i.e., IS−SI triblock copolymers) should have no significant influence on the dynamics of the spherical micelles, since it does not change the micellar structure itself.[18]

The block copolymer was labeled in pure THF, using a crown ether (18-crown-6) to dissolve the cesium salt of the photoreactive dye in the organic solvent THF. Cesium iodide was added to enhance the coupling efficiency by exchanging the chlorine of the chloromethyl group. The labeling efficiency, determined by UV−vis absorption, exceeded by 50% that of the total diblock copolymer, and by more than 70% that of the chloromethyl functionalization (determined by NMR) of the diblock copolymer. Labeled polymers were purified by precipitation of the labeling solution into methanol and careful rinsing of the precipitate with a cold 50/50 wt % water/methanol mixture. To remove excess amounts of uncoupled dye molecules, which would disturb the FRS diffusion measurements, the labeled block copolymer was reprecipitated three times from THF solution. Total removal of the free dye from the block copolymer was confirmed by GPC, using a UV−vis absorption detector at the absorption maximum wavelength (i.e., 432 nm) of the dye label.

Table 1. Characteristics of the Homopolymer and Block Copolymer

sample code	M_n	M_w/M_n	wt % PS
SI	64 800	1.04	20.7
PI	47 900	1.03	0

Table 2. Composition of Block Copolymer/Homopolymer Blends

specimen	wt% SI	wt% PS	specimen	wt% SI	wt% PS
SI-10	12.1	2.5	SI-40	40.0	8.3
SI-20	22.7	4.7	SI-50	50.7	10.5
SI-30	29.7	6.1			

As matrix homopolymer for the block copolymer/homopolymer blends, polyisoprene of molecular weight comparable to that of the PI block of the block copolymer was synthesized by living anionic polymerization under the same conditions as for preparation of the diblock copolymer. A summary of the sample characteristics is given in Table 1.

Block copolymer/homopolymer blends with spherical microdomains at intermediate brush conditions, i.e., the block copolymer corona only slightly swollen by the homopolymer, were prepared by solvent casting of a mixture of SI and PI from cyclohexane. To lower the label content of the micelles, a 50/50 wt % mixture of labeled SI and nonlabeled SI was used. The solution was poured into Teflon dishes and left standing at room temperature for slow evaporation of the solvent. As-cast films were annealed for 3 days under vacuum at $T = 110$ °C, slightly above the glass transition of the PS cores. All block copolymer/homopolymer blends contained 0.5 wt % 2,6-di-*tert*-butyl-4-methylphenol (BHT) to stabilize the PI against cross-linking by oxygen. Table 2 gives an overview of the sample composition of all samples, which will be discussed in the following sections.

Small-Angle X-ray Scattering. SAXS measurements described in this paper were conducted with a setup using a rotating anode X-ray generator (18 kW, MAC-Science Co. Ltd., Yokohama, Japan), a graphite monochromator for monochromatization of the incident beam, and a one-dimensional position-sensitive proportional counter (PSPC) as detector. The wavelength of the radiation was 0.154 nm (Cu Kα), the camera length 1988 mm. All scattering profiles were corrected for absorption of X-ray radiation by the sample, air-scattering, and slit-smearing effects prior to data fitting.

Forced Rayleigh Scattering. Self-diffusion coefficients of dye-labeled spherical micelles in a homopolymer melt have been determined using a standard FRS setup as described elsewhere.[23] In the first step, the sample is exposed to two coherent interfering laser beams from an Ar^+ laser operating at a wavelength of 488 nm with a light intensity of 100 mW. During this period, a holographic diffraction grating is created by photobleaching of the dye labels at the position of the interference maxima. The typical exposure time is 25 ms. Next, one of the laser beams is shut off and the other is attenuated by a factor of 10^4 to avoid further photobleaching of the specimen. The Bragg diffraction of the attenuated beam then is recorded as a function of time, using a photomultiplier in the position of the first-order Bragg peak. Due to diffusional motion of the dye-labeled particles, the amplitude of the holographic grating decreases with time. Consequently, the diffracted signal intensity also decays. In the case of one simple translational diffusion process, this signal decay is described by

$$I(t) = [A \exp(-t/\tau)]^2 + C \qquad (2)$$

A is the amplitude of the diffraction signal immediately after photobleaching, τ the diffusional relaxation time, and C the scattering background contributing incoherently to the FRS intensity and therefore identical to the scattering measured before photobleaching. The translational self-diffusion coefficient D_s is determined from the relaxation time according to

$$D_s = d^2/4\pi^2\tau \tag{3}$$

Here, d is the periodic lattice spacing of the holographic grating, which depends on the wavelength λ of the laser and the bleaching angle 2θ:

$$d = \lambda/(2 \sin \theta) \tag{4a}$$

$$q = 2\pi/d \tag{4b}$$

q is the length of the scattering vector of the FRS experiments. Its magnitude is proportional to $\sin \theta$, and therefore reciprocal to the holographic lattice spacing d.

FRS samples were prepared at room temperature by cold pressing between two optical disk-shaped glass plates with diameter 2 cm. The sample thickness was adjusted to 0.1 mm by Teflon spacers. All samples were annealed at the measurement temperature for 6 h prior to the first diffusion measurement. This annealing period allows for relaxation of convectional or pressure-induced flow processes, which lead to regular oscillations in the FRS decaying signals.

Mechanical Spectroscopy. Dynamic mechanical measurements have been performed using a Rheometrics RMS 800, with plate−plate geometry and variable plate diameters (6 and 13 mm). The samples were subjected to small oscillatory shear strain, and the resulting stress was measured. Master curves for the real (G') and imaginary (G'') parts of the dynamic complex shear modulus have been obtained using the time−temperature superposition principle (i.e., shifting the data recorded at various temperatures only along the frequency coordinate).[24] For this purpose, samples have been measured in the temperature range -60 °C $< T <$ $+120$ °C, where the micellar core still should be kinetically fixed. Consequently, the structure of the SI/PI blend containing spherical micelles should remain unchanged in this regime, as has been confirmed previously by SAXS measurements.[7,18] The mechanical measurements have been used to determine relaxation times of the characteristic relaxation processes observed in various systems within the range between the segmental relaxation and the terminal flow. To separate the partially overlapping relaxation processes observed in the terminal relaxation range, the frequency dependencies of the dynamic moduli have been transformed to time dependencies of the relaxation modulus $G(t)$. The latter dependencies have been fitted with a sum of stretched exponential functions, the number of components corresponding to the number of clearly distinguishable relaxation modes.

Dielectric Spectroscopy. Dielectric measurements have been performed using a setup with the Solartron-Schlumberger FRA 1260 frequency response analyzer and a condenser cell, allowing the frequency range between 10^{-2} and 10^6 Hz to be analyzed. The complex dielectric modulus $M^*(\omega) = M'(\omega) + iM''(\omega)$ has been determined at various temperatures, and similarly to that in the case of the mechanical results, a master curve has been constructed by only a horizontal (frequency) shift of the data. Positions of maxima of $M''(\omega)$ have been considered as determining the relaxation times of corresponding relaxation processes.

Results and Discussion

Structure Analysis by SAXS. Examples of the small-angle X-ray scattering intensity profiles recorded for samples containing various amounts of the block copolymer are shown in Figure 1. Qualitatively, the detected scattering profiles can be considered as typical for spherical microdomains with some correlation of interdomain distances. The particle form factor peaks

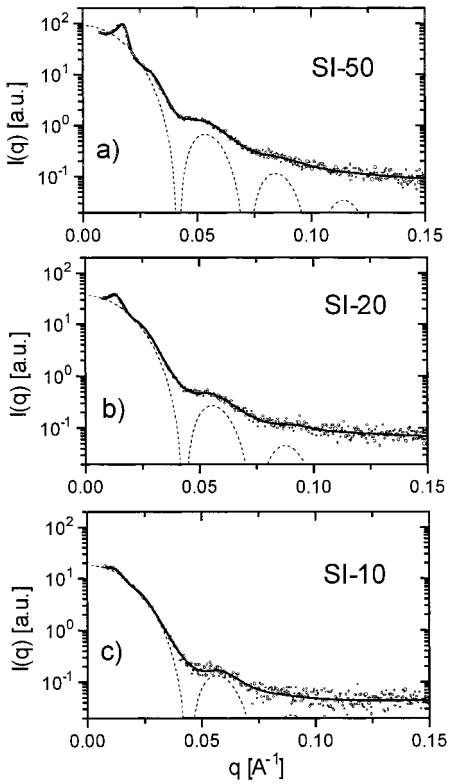

Figure 1. SAXS intensity distributions recorded at room temperature for block copolymer/homopolymer blends of various compositions. The solid lines represent the best fits of the paracrystalline model (fit parameters are given in Table 3). The dashed lines illustrate the particle form factor of the spherical cores of the micelles.

for spherical objects (dashed lines) are seen in all cases, independently of block copolymer concentration. Therefore, formation of almost identical spherical micelles in the blends can be assumed for the whole concentration regime. On the other hand, the interparticle structure peak at low q appears to be influenced by the copolymer concentration, indicating a considerable effect of concentration on the correlation of the interparticle distances. The height and sharpness of the interparticle correlation peak strongly decrease with decreasing concentration, which corresponds to an increase of disorder. Whereas, at 50 wt %, particles show a structure with well-correlated particle distances, the correlation almost disappears at 10 wt %, and this state corresponds to a fluid phase also found for colloidal hard sphere particles at lower concentrations.[1]

In spite of the very limited order between the micelles in the blends, the SAXS data have been analyzed using the paracrystalline fitting method[25] rather than by simply evaluating the peak positions. The paracrystalline fitting method is used to calculate trial SAXS profiles assuming a certain particle shape and interparticle arrangement. Examples of the fits are shown in Figure 1 by solid lines. In the case of spherical micelles on a cubic lattice, fitting parameters are the edge of the cubic lattice a, the lattice distortion $\Delta a/a$, the type of the cubic lattice (SC, FCC, or BCC), the micellar core radius r, radius polydispersity $\Delta r/r$, and the interface roughness. These characteristic structural parameters of our systems and typical propositions between them are illustrated in Figure 2. Here, d is the interparticle spacing of nearest neighbors, corresponding to the position of the maximum in the structure

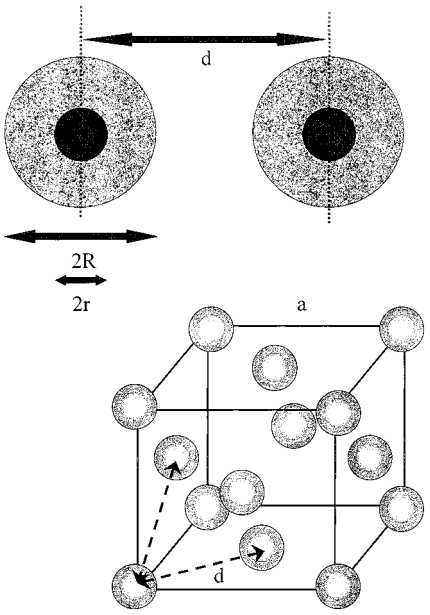

Figure 2. Schematic illustration of micelle sizes and distances between micelles in a blend.

Table 3. Fit Parameters for Block Copolymer/ Homopolymer Blends with Various Block Copolymer Concentrations, Obtained from a Paracrystalline Fitting Model

specimen	r (nm)	$\Delta r/r$	a (nm)	$\Delta a/a$
SI-50	10.8	0.14	48.0 (BCC)	0.14
SI-20	10.4	0.14	63.5 (BCC)	0.21
SI-10	10.2	0.14	84.0 (FCC)	0.35

factor (see Figure 1). The structural parameters obtained as a result of the fitting procedure for various compositions of the blends are summarized in Table 3.

The results show that, whereas the size of single micelles remains nearly constant, there is a considerable increase of the lattice distortion parameter with decreasing micelle concentration. At a concentration of 10 wt % of the block copolymer, the lattice distortion is larger than 30%, which makes the usage of the paracrystalline model for such low micelle concentrations questionable. Nevertheless, the paracrystalline model allowed us to quantify the differences in ordering between various samples and to confirm that the micellar structure itself remains unchanged in the concentration regime studied. A more detailed discussion of the interparticle structure based on the scattering signals is beyond the scope of this paper.

Comparing the interparticle spacing as determined by SAXS with the total micellar radius, i.e., $R = r_{core} + l_{corona} = 28.5$ nm (with $l_{corona} = 18$ nm for unperturbed chain dimensions of PI ($M = 51\,000$)), we find that individual micelles should start to interpenetrate slightly at block copolymer concentrations larger than 20 wt %. Alternatively, the corona chains might be compressed compared to the unperturbed dimensions. Here, it should be noted that this compression has to be about 20% in length for the blend with 30 wt % SI (SI-30) and up to 35% for sample SI-40, if we assume that individual micelles do not yet overlap in the regime $c_{SI} < 40$ wt%. The true structure of the corona chains of the copolymer micelles in the homopolymer melt, which cannot be determined from our SAXS analysis, will be resolved by small-angle neutron scattering in the near future.

Finally, besides the determined structural parameters discussed above, the average number of block copolymer chains per micelle can be calculated considering the volume of the micellar cores determined by SAXS and the molecular weight of the PS block determined by GPC. This simple calculation, taking into account the bulk density of PS as 1.053 g/cm^3 and assuming an average PS core radius of 10.6 nm, leads to an average of about 250 block copolymer chains per micelle as representative for all concentrations.

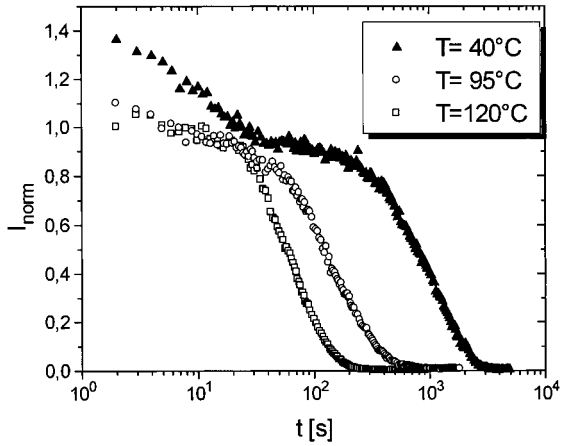

Figure 3. Typical FRS correlation functions, obtained from sample SI-10 at diffraction angle $2\theta = 30°$.

FRS−Diffusion Studies. To estimate interparticle interactions and their role on self-diffusion for spherical micellar systems, intermediate brush systems with various micelle concentrations in the range 10−50 wt % have been investigated by FRS. In Figure 3, typical FRS decays for a sample containing 12.1 wt % spherical micelles obtained for different temperatures are shown. Opposite to samples with very high micelle concentrations of 50 wt %, where strange decay−grow−decay signals previously have been found,[18] these signals show a monotonous decay. At sample temperature $T = 40$ °C, two relaxational processes clearly can be distinguished. Recently, two processes also have been found by FRS diffusion measurements of glassy spherical micelles in a nonentangling homopolymer matrix.[19] However, the authors have not been able to give a definite explanation for the origin of the fast relaxational process. Here, this fast process is identified as rotation of spherical micelles, as will be shown further below. The slow process corresponds to micellar translational diffusion. At higher temperatures, the fast process decays too fast for the time resolution of the FRS experiment, where signals show a monoexponential decay.

Signals showing two relaxation processes (see Figure 3) could not be analyzed by the simple eq 2, but had to be fitted by a biexponential decay according to

$$I(t) = [A_1 \exp(-t/\tau_1) + A_2 \exp(-t/\tau_2)]^2 + C \quad (5)$$

A_1 is the amplitude of the rotational diffusion process and A_2 the amplitude of the translational process. τ_1 and τ_2 are the rotational and translational relaxation times, respectively. Whereas the translational relaxation time scales with q^2 (see above), rotation corresponds to a localized relaxation of the holographic lattice and should be independent of the lattice dimensions $d \approx 1/q$.

To determine the nature of the two relaxation processes, the dependence of the relaxation rates on the lattice spacing $d \approx 1/q$ has been analyzed. As an example, the resulting relaxation times for a sample

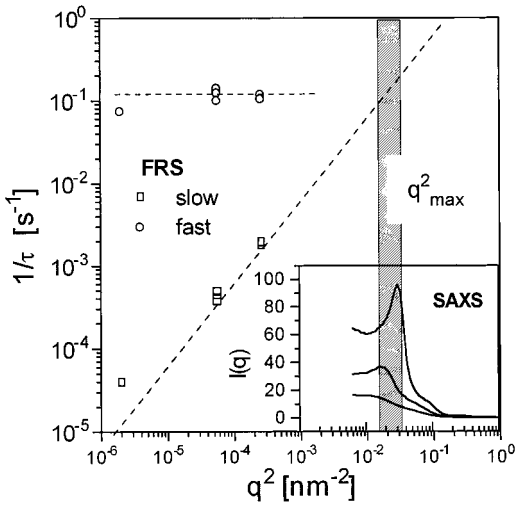

Figure 4. Relaxation times $1/\tau$ vs q^2 determined from FRS measurements at $T = 40$ °C. The inset shows scattered intensity profiles recorded for various samples. The shadowed area indicates the q range corresponding to the intermicellar correlation distances.

containing 12.1 wt % block copolymer (Si-10) have been plotted versus q^2 in Figure 4. In addition, the structure factors $S(q)$ as determined by SAXS (see Figure 1) have also been sketched, emphasizing the q scale of the intermicellar structure with respect to the experimental q scale of the FRS diffusion experiments. Whereas the faster process, corresponding to the smaller relaxation time, seems to be independent of q, the slower process scales linearly with q^2. Therefore, the fast process clearly is related to a localized relaxation process or rotation. The slow process corresponds to translational diffusion of the spherical micelles, as claimed above.

Here, it should be noted that localized processes such as rotation may contribute to the FRS signal for the following reason: the incident laser beams are linearly polarized, and the bleaching process is mainly restricted to photolabels whose transition momentum is oriented almost parallel to the polarization direction of the incident light. Especially if the rotational relaxation time of the tracers is much longer than the bleaching period, this leads to a photoselection process. Immediately after photobleaching, the bleached areas of the sample show no light absorption of the polarized reading beam. However, independent rotation of labeled tracers leads to randomization of the orientations of the nonbleached labels within the bleached areas. Therefore, the absorption in these areas increases, and consequently the contrast of the overall diffraction grating decreases as a function of time. From the corresponding relaxation rate, which should be independent of lattice spacing, a rotational diffusion coefficient of the labeled species can be determined.[18]

In Table 4, we have summarized the rotational relaxation times τ_{rot} and self-diffusion coefficients D_s for block copolymer/homopolymer blends with various block copolymer concentrations, obtained from FRS measurements at three different temperatures. Values for sample SI-50 are not given in the table, because this highly concentrated micellar system exhibited unusual decay−grow−decay FRS signals, which are still not perfectly well understood. The interested reader is refered to ref 18, where a scenario plausibly explaining these unusual signals is described.

Table 4. Rotational Relaxation Times and Self-Diffusion Coefficients for Block Copolymer/Homopolymer Blends with Various Block Copolymer Concentrations, Obtained from FRS Measurements at Three Different Temperatures

specimen	τ_{rot} (s)	D_s (40 °C) (cm^2 s^{-1})	D_s (95 °C) (cm^2 s^{-1})	D_s (120 °C) (cm^2 s^{-1})
SI-10	9.4	6.9×10^{-14}	7.6×10^{-13}	2.0×10^{-12}
SI-20	5.5	8.0×10^{-14}	5.1×10^{-13}	1.4×10^{-12}
SI-30	17.0	1.1×10^{-14}	2.5×10^{-13}	1.1×10^{-12}
SI-40	13.8	5.9×10^{-14}	0.9×10^{-13}	0.8×10^{-12}

The values for τ_{rot} show no systematic variation with increasing micellar concentration, which emphasizes that the micelles do not yet interpenetrate up to 40 wt % block copolymer concentration. Therefore, individual micelles rotate independently of each other, and this relaxation process is mainly determined by the size of the micelle and the viscosity of the homopolymer matrix. Assuming an average τ_{rot} of 10 s for samples SI-10 to SI-40 and using the Debye equation (eq 6), one can

$$\tau_{rot} = 4\pi\eta R_{rot}^3/3kT \qquad (6)$$

determine the hydrodynamic radius R_{rot} of the rotating micelle. In eq 6, η is the viscosity of the matrix, which has been measured as 413.8 Pa s at $T = 40$ °C for our PI. These values yield an effective radius $R_{rot} \approx 29$ nm, which is in good agreement with the dimensions of a single micelle as determined by SAXS ($R_{rot} = r_{PS\ core}$ (10.5 nm) + $r_{PI\ corona} = 28.5$ nm (see above)). Whereas the rotation of individual micelles seems to be independent of micelle concentration and is determined only by the viscosity of the matrix homopolymer at block copolymer concentrations $c < 40\%$, the translational diffusion D_s shows a strong dependence on micelle concentration even in this regime, as also expected for hard sphere colloidal particles.[1]

Finally, it should be noted that D_s for sample SI-40 at $T = 40$ °C is comparatively fast, i.e., similar to the values obtained for the more dilute samples SI-20 and SI-10. At higher $T = 95$ or 120 °C, D_s decreases monotonously with increasing concentration as expected. This effect previously has been ascribed to the photoselection of highly mobile micelles and/or isolated block copolymer chains in a structurally heterogeneous system[18] at low temperatures. The concentration dependence of D_s in the normal regime, i.e., samples SI-10 to SI-30, where individual micelles should not or only slightly interpenetrate, will be discussed in some detail in the next section.

Concentration Dependence of Diffusion of Micelles in a High Molecular Weight Homopolymer Matrix Compared to a Low Molecular Weight Matrix. In Figure 5, we compare the concentration dependence of D_s, in the regime where the corona of individual micelles should not yet interpenetrate, for our system with studies of the dynamics of styrene−isoprene block copolymer micelles embedded in a matrix polyisoprene of very low molecular weight ($M = 4100$).[19] The line indicates the behavior expected for hard sphere colloids.[1] Whereas the diffusion data for micelles in a nonentangling polymer matrix[19] depend more strongly on micellar concentration than expected for hard sphere systems in the same concentration regime, our intermediate brush system in the entangled matrix shows hard sphere behavior,[1] i.e., $D_s \approx 1 - 2c$, for moderate concentrations. The system studied in ref 19 was

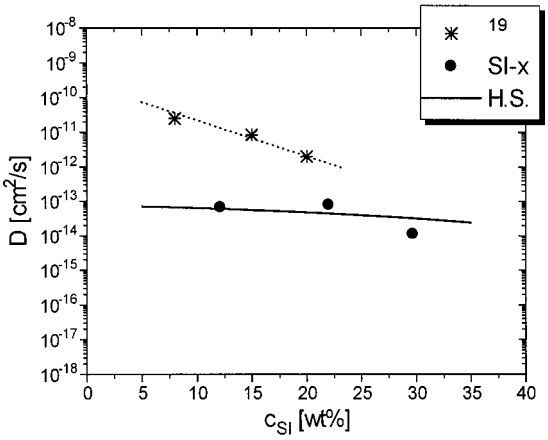

Figure 5. Comparison of the concentration dependence of self-diffusion coefficients of block copolymer micelles in an entangled homopolymer matrix with results for a system of strongly swollen block copolymer micelles in a nonentangling homopolymer matrix of very low molecular weight.[19] The dashed line is a guide to the eye. The solid line indicates the well-known behavior of hard sphere colloids[1] ($D \approx (1 - 2c)$).

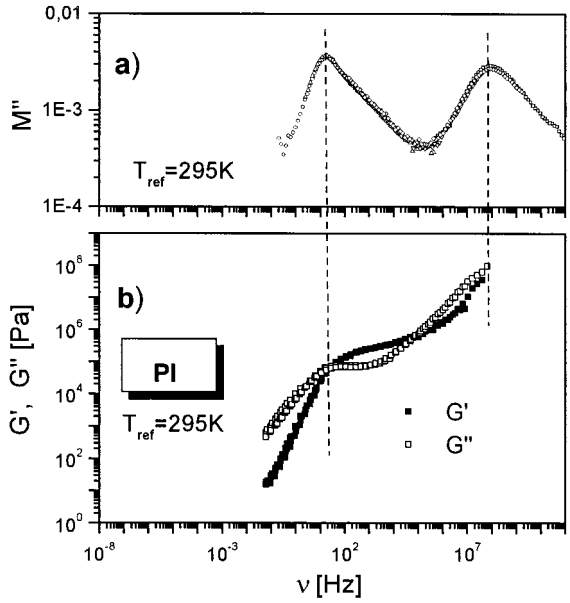

Figure 6. Frequency dependencies of (a) the imaginary part of the dielectric modulus M'' and (b) the components of the complex shear modulus (G', G'') for the polyisoprene homopolymer melt at indicated reference temperatures. Vertical dashed lines indicate the frequencies corresponding to the characteristic segmental and chain relaxation processes.

embedded in a very short chain PI matrix. Therefore, the corona of the block copolymer micelles is expected to be strongly swollen by the matrix homopolymer. As a consequence, the range of intermicellar interactions increases in comparison to intermediate or dry brush systems with less swollen corona,[5] and the effective hard sphere volume fraction is considerably larger than the block copolymer concentration itself. Correspondingly, in an identical micellar concentration regime wet brush micelles are always expected to show a stronger dependence of particle mobility on concentration compared to systems with less swollen corona and interparticle interactions of shorter range.

Another important result concerns the difference in absolute magnitude of diffusional data shown in Figure 5. The radii of the spherical micelles are nearly identical (8 nm for the wet brush PS cores,[19] 10.6 nm for the intermediate brush system (see Table 2)). In the dilute regime, where micelles do not interentangle, according to Watanabe[16] the particle diffusivity should be determined by the micellar radius and the viscosity of the homopolymer matrix. Therefore, the wet brush and intermediate brush micelles of equal size should differ in particle mobility by the same factor as the respective PI matrix viscosities. Unfortunately, the matrix viscosity of the short-chain PI used in ref 19 has not been mentioned. However, since the molecular weight was close to the entanglement molecular weight of PI (M_e = 5.000); the viscosity of the short-chain PI should be at least by a factor of $(49/5)^{3.4} \approx 2000$ smaller compared to the matrix homopolymer used for our intermediate brush samples (M = 49 000). The temperature difference of 10 °C (intermediate brushes, 40 °C; wet brushes,[19] 30 °C) is neglectable. Therefore, diffusion coefficients of our intermediate brush micelles should be more than 3 decades smaller than the diffusion coefficients of the wet brush system. Whereas this relation is fulfilled if the diffusion data are interpolated to zero micellar concentration, the difference becomes smaller with increasing particle concentration. Like found in rheological measurements,[16] the diffusion coefficients of spherical micelles with respect to the matrix viscosities are much faster for the entangling matrix than for the short-chain nonentangling matrix. However, for ideally dilute systems without any intermicellar interactions, the micellar mobility seems to scale nicely with the viscosity of the homopolymer matrix. Therefore, the differences at higher particle concentrations may depend only on the difference in interparticle interactions of wet, intermediate, and dry brush micelles, as discussed before. This may explain the earlier findings of Watanabe and co-workers, who, in rheological studies of block copolymer micelles in an entangling matrix in the moderately concentrated regime, always found a faster terminal relaxation process than expected by the Stokes−Einstein equation. These results also provide a nice illustration of how the interparticle interactions of block copolymer micelles in a block copolymer/homopolymer blend can be tuned via the molecular weight of the homopolymer matrix.

Dielectric and Mechanical Relaxation Behavior. Before presenting results for the copolymer/homopolymer mixtures, we illustrate the behavior of the pure components as observed by the two relaxation spectroscopy methods. Figure 6 shows typical dielectric and mechanical results obtained for the polyisoprene melt. Two distinct relaxation processes are observed by means of both methods. They are attributed to the segmental and polymer chain relaxations as observed at high and low frequencies, respectively. The bulk copolymer sample SI is characterized by means of the results shown in Figure 7. Two processes similar to those for the PI homopolymer are seen for the copolymer, as well. In this case, they correspond to the segmental relaxation of the polyisoprene units (high frequency) and to the polyisoprene block relaxation in the microphase-separated system (low frequency). Although the polyisoprene forms a continuous liquid matrix for the glassy PS microdomains, the copolymer sample does not flow at frequencies smaller than those corresponding to the polyisoprene block relaxation; i.e., no terminal relaxation process has been found besides the two relaxation processes attributed to the polyisoprene block chains.

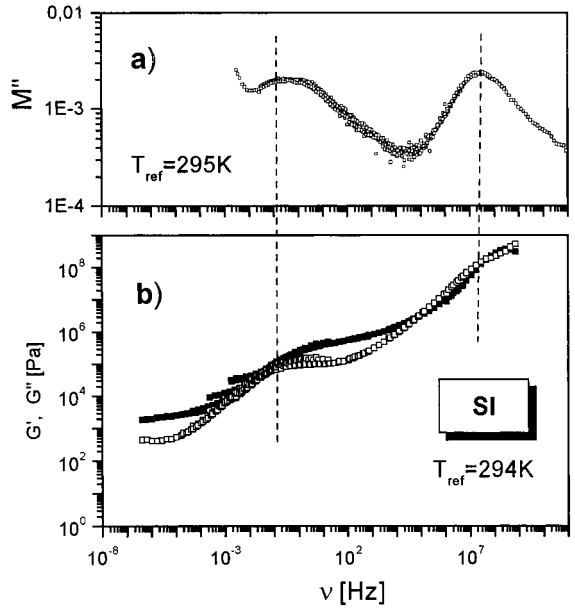

Figure 7. Frequency dependencies of (a) the imaginary part of the dielectric modulus and (b) the components of the complex shear modulus for the styrene−isoprene block copolymer at indicated reference temperatures. Vertical dashed lines indicate the segmental and block relaxation processes of the isoprene component.

This indicates either a highly ordered phase of block copolymer micelles or a different microphase structure. In any case, the structural arrangement of the PS microdomains is maintained during our rheological experiments, resulting in a clear G' plateau in the low-frequency range for this sample. Macroscopic flow of the sample might be induced only by an increase of temperature above that of the presented measurements, where the microdomain structure could change to a more disordered state.

An example of the relaxation behavior of the homopolymer/copolymer mixtures is shown in Figure 8. As in the two former cases, the two relaxation processes (the PI segmental relaxation and the relaxation of PI chains or blocks) are also detected in the mixtures at characteristic frequencies. In the mixtures, however, additionally a low-frequency relaxation is observed which partially overlaps with the PI chain relaxation for small copolymer concentrations, but becomes well separated for higher copolymer content in the system. The appearance of this process is well correlated with the development of order between block copolymer micelles dispersed in the homopolymer matrix and might be attributed to a structural relaxation involving translational rearrangements of a certain number of micelles. This slow relaxation controls the crossover to the terminal Newtonian flow regime of the mixture. Therefore, it must be related to the onset of the global micellar mobility and can be regarded as the colloidal α-relaxation. The mechanical response of the sample shown in Figure 8 is to a large extent analogous to the behavior observed for ordered melts of multiarm stars.[26]

The temperature dependencies for the relaxation rates of various samples as determined by dielectric (DS) and mechanical (MS) relaxation spectroscopy are presented in Figure 9. Figure 9a shows these dependencies for the pure components. The same segmental relaxation rates (τ_s) for polyisoprene are observed in both components, whereas a small difference between

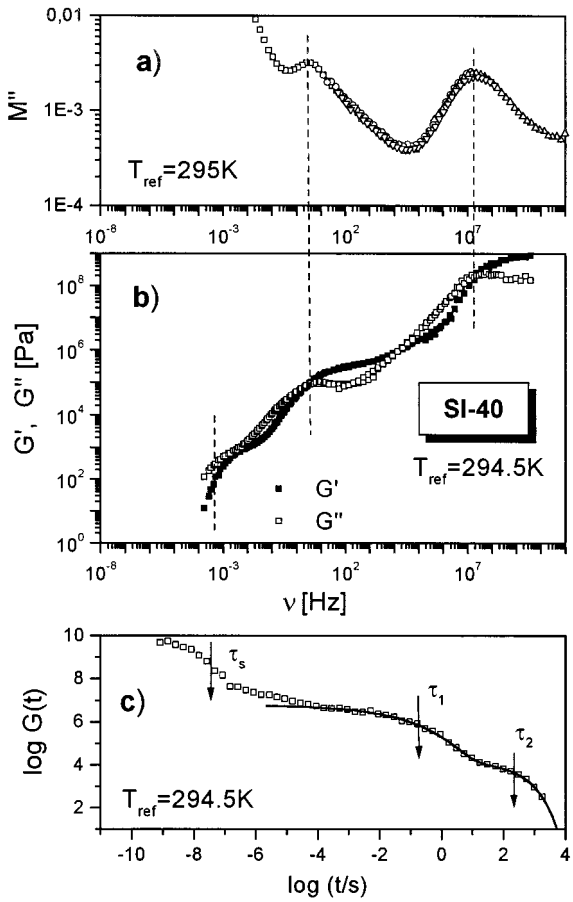

Figure 8. Frequency dependencies of (a) the imaginary part of the dielectric modulus and (b) the components of the complex shear modulus for the blend of styrene−isoprene block copolymer and polyisoprene at indicated reference temperatures. Vertical dashed lines indicate the PI segmental (τ_s), PI chain (τ_1), and structural relaxation (τ_2) processes. In (c) the relaxation modulus $G(t)$ is shown as determined from the dynamic mechanical results presented in (b). The solid line in (c) represents the best fit of the sum of two stretched exponential decays, used to determine τ_1 and τ_2.

relaxation rates corresponding to chains in the polyisoprene melt (τ_1) and to polyisoprene blocks in the microphase-separated copolymer (τ_b) is observed. Here, it also should be noted that τ_b as determined by MS is slightly larger than the relaxation time measured in the dielectric experiments, a phenomenon which is not yet understood.

In Figure 9b, the relaxation times detected in blends of various compositions are shown in comparison with the relaxation times of the pure polyisoprene matrix (see Figure 9a). The results indicate that the two matrix processes τ_s and τ_1 appear as almost unchanged in the blends and are not influenced by the blend composition. Besides them, as already shown in Figure 8, an additional relaxation in the terminal zone (τ_2) appears which exhibits a clear dependence on composition. In the regime of copolymer concentrations up to 40%, the increasing micelle concentration involves a slight slowing of this process, but the increase of micelle concentration above 40% involves a drastic increase of the slowest relaxation time. In Figure 9b, diffusional relaxation times determined by FRS for sample SI-20, recalculated according to eq 3 for two different length scales $q = 2\pi/2r$ (corresponding to the micelle core dimension) and $q = 2\pi/d$ (corresponding to the inter-

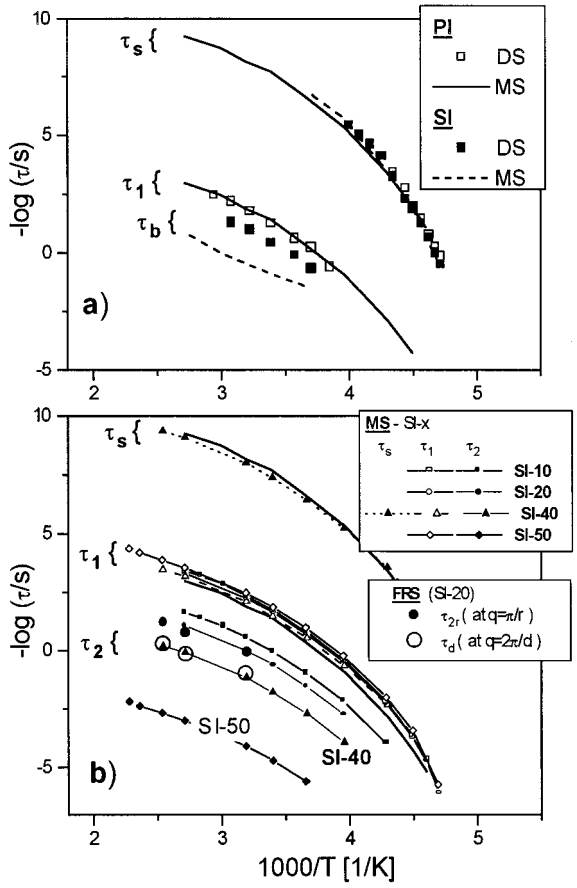

Figure 9. Activation plots (relaxation times vs 1000/T) for various relaxation processes determined using various methods for various samples: (a) relaxations in the pure components of the blends as detected by mechanical and dielectric spectroscopy and (b) relaxations in blends of various compositions in comparison with the relaxations in the matrix (fat solid lines).

micellar spacing), have also been included. The relaxation rates of diffusion on a length scale comparable to the micellar dimension (τ_{2r}) correspond much better to the dynamical mechanical results (τ_2), as will be discussed in more detail in the next section.

Comparison of the Mechanically Detected Relaxations with the Diffusion Rates. To compare the mechanically detected relaxation rates for the blends with the diffusion rates of micelles determined by means of FRS, the q-dependent relaxation times from FRS have been extrapolated to the q range corresponding to micellar sizes $2r$ and to intermicellar distances d as described above. An example of such comparison has already been shown in Figure 9b, where the solid circles represent diffusional relaxation times at q corresponding to the micelle core dimensions ($2r$), and the open circles represent the times at q corresponding to the mean intermicellar distance (d) for the same sample SI-20. It has been found that the mechanical terminal relaxation times correlate better with the diffusional relaxation corresponding to the size of individual micelles. This suggests that the mechanically detected slow relaxation should rather be considered as "form" or rotational relaxation of a single micelle and not as a cooperative structural rearrangement of ordered micelles. In the case of a structural rearrangement the mechanical relaxation should correspond to the diffusional relaxation related to intermicellar distances d.

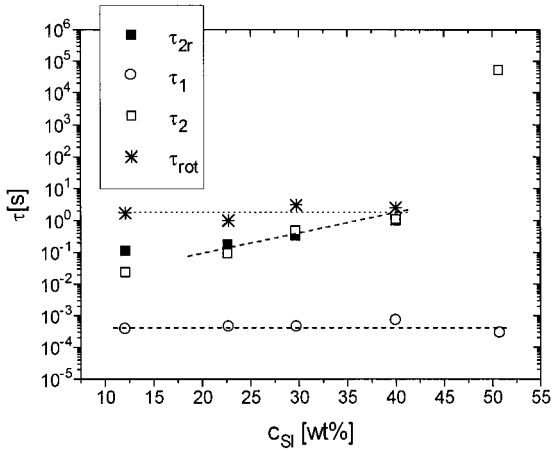

Figure 10. Comparison of the mechanical relaxation rates, τ_1 and τ_2, determined for blends of various compositions, with relaxation rates τ_{2r} and τ_{rot} determined by FRS. The FRS relaxation times corresponding to translational diffusion, τ_{2r}, have been rescaled for the scattering vector q corresponding to the micellar core dimensions $2r$.

Finally, in Figure 10 the concentration dependencies of relaxation rates determined by FRS and mechanical spectroscopy for block copolymer micelles in an entangled homopolymer melt are compared. Whereas τ_1, attributed to chain relaxation of the polyisoprene block and/or the PI matrix chains, is independent of block copolymer concentration (see above), τ_2 and τ_{2r} show a slight increase with concentration up to $c_{SI} = 40$ wt %. These two relaxation rates attributed to dynamics of individual micelles agree extremely well in this concentration regime, as already shown above for sample SI-20 (see Figure 9b). The situation changes at higher compositions when the micelles form higher correlated structures with individual micelles strongly caged between neighbors, which excludes individual diffusion and involves a necessity of cooperative rearrangements with a considerably longer relaxation time. This strong slowing of the terminal relaxation has been observed by MS for the composition of 50 wt % SI (sample SI-50), as shown in Figure 10. Unfortunately, τ_2 could not yet be compared to FRS measurements for this highly concentrated sample due to the unusual decay−grow−decay signals found in this case. These signals previously had been attributed to a superposition of the diffusion of mobile micelles within liquid-like regions and an ultraslow structural rearrangement of highly ordered micellar regimes, all within a structurally heterogeneous sample.[18] The fast process of these FRS signals yields a similar relaxation time for samples SI-40 and SI-50, which clearly indicates a conceptional difference of the diffusional processes detected for these two samples. The ultraslow mode might correspond to $\tau_2 = \tau_d$ for the sample SI-50. However, in this case the fastest possible FRS relaxation time (taking the shortest possible length scale of the FRS experiment, i.e., $l =$ 300 nm) would be on the order of 5×10^6 s, which is beyond the experimental capability. In conclusion, the comparison of FRS and MS for highly concentrated micellar systems as sample SI-50 is not possible in the current state for the reasons stated above.

Interestingly, the rotational correlation times determined by FRS, which are independent of block copolymer concentration, are even slightly slower than the diffusional relaxation times, τ_2 and τ_{2r}, up to a crossover concentration of 40 wt %. This seems to further empha-

Table 5. Translational Diffusion Coefficients (See Table 4), Terminal Relaxation Times (See Figure 10), and Resulting Diffusion Distances at Reference Temperature $T = 95$ °C

specimen	D_s (cm^2 s^{-1})	τ_2 (s)	δ (nm)
SI-10	7.6×10^{-13}	0.0223	3.2
SI-20	5.1×10^{-13}	0.0863	5.1
SI-30	2.5×10^{-13}	0.475	8.4
SI-40	0.9×10^{-13}	1.13	7.8

size that the terminal relaxation found in mechanical spectroscopy is mainly caused by a rather localized motion of individual micelles than by a structural rearrangement over a length scale comparable to the intermicellar distance d. Here, it should be noted that the fact that $\tau_{rot} > \tau_{2r}$ does not indicate that micelles are diffusing over a considerable distance without rotation. $2r$ is the q scale of the FRS experiment (see eq 4), while the diffusion distance of the tracer particles itself has to be calculated according to

$$\delta = (6D\tau)^{0.5} \tag{7}$$

Comparing eqs 7 and 3, it is simple to show that a holographic lattice constant of $2r = 20$ nm corresponds to a diffusion distance of $2r/(2\pi/6^{0.5}) = 7.7$ nm, i.e., even smaller than the micellar core radius. On the other hand, if we calculate the diffusional distance during the rotational relaxation time for sample SI-10 (see Table 4) at $T = 95$ °C by using eq 7, we obtain $\delta = 26$ nm. Therefore, for dilute samples, particle diffusion and rotation are comparable concerning their typical length scale, which is close to the radius of the total micelle. For systems with higher micelle concentration, the diffusional length scale with respect to the rotational length scale decreases.

Finally, we have determined the diffusional length scale corresponding to the terminal relaxation rate τ_2. The results are summarized in Table 5, using a reference temperature of 95 °C. With increasing concentration, the diffusion distance converges to the core radius of the micelles. These findings are in qualitative agreement with the recent results for the dynamics of micelles in a nonentangled homopolymer melt by Watanabe et al.,[19] who also found that the terminal relaxation process corresponds to diffusion over a length scale comparable to the micellar core dimensions. Interestingly, our data indicate a systematic increase of this diffusion distance with increasing concentration. For very dilute samples SI-10 and SI-20, our diffusion distance is much smaller compared to the previous findings by Watanabe et al.[19] This may be caused by the fact that our micelles are less swollen and therefore only show weak interparticle interactions. Also, the entanglements of the matrix polymer might lead to a slowing of particle diffusion with respect to mechanical relaxation. A more systematic study of the effect of the molecular weight of the matrix homopolymer on the concentration dependence of relaxation rates determined by FRS and MS currently is in progress.

Conclusions

In this paper, studies of the dynamics of spherical block copolymer micelles in an entangled homopolymer melt by forced Rayleigh scattering, rheology, and dielectric relaxation spectroscopy have been presented. To fix the micellar structure, glassy spherical micelles with a PS core and PI corona have been investigated. The microstructure of this system is quite similar to that of surfactant micelles in aqueous dispersions. However, our micelles are kinetically frozen and therefore can show no exchange of individual block copolymer chains between micelles. In addition, most aqueous surfactant molecules contain highly polar groups or even charges. Therefore, the intermicellar interactions may become quite complicated, whereas our nonpolar micelles simply should show sterical interparticle interactions.

For these micellar systems with intermediate brush architecture, a biexponential FRS decay was observed at very low temperature. The fast process has been attributed to rotational diffusion, which has been proved by the q dependence of the relaxation rate. Diffusion coefficients have been compared with rheological studies, and with recent FRS measurements of wet brush block copolymer micelles in a nonentangling PI matrix. Results shown here indicate a strong increase in the range of repulsive interactions of spherical micelles with increasing swelling of the micellar corona. This strong effect of matrix molecular weight on intermicellar interactions may be the reason for the difference in rheological behavior of spherical micelles in a nonentangling and an entangling homopolymer matrix at moderate block copolymer concentration, where the terminal relaxation process attributed to micellar diffusion has been found to be comparatively faster in the case of the entangling matrix.

Mechanical relaxation spectroscopy of the block copolymer/homopolymer blends revealed three relaxational processes. The fast processes have been attributed to segmental relaxation and to chain relaxation of the polyisoprene block and the matrix homopolymer, which has been confirmed independently by dielectric spectroscopy. The terminal relaxation process has been attributed to relaxation of individual micelles. In comparison with the FRS measurements, the diffusional length scale of the terminal process has been found to correspond to the micellar dimensions. At very high concentrations, where individual micelles should strongly overlap and form a highly ordered structure, a large increase of the terminal relaxation time has been found. Unfortunately, these highly concentrated samples yielded unusual FRS signals. Therefore, the diffusional length scale of the terminal process in this concentration regime could not yet be determined and remains an important and interesting problem for future studies.

Finally, it should be noted that it is also possible to study the inverse system, i.e., micelles with a PI core and PS corona in a PS melt. This system is very interesting because it allows for chemical cross-linking and thereby fixation of the micellar structure, a possibility which currently is investigated. Those cross-linked micelles could be isolated, and their dynamics could therefore be studied even well below the critical micellar concentration.

Acknowledgment. We thank Ms. Y. Kanazawa, ERATO Polymer Phasing Project, for synthesis of the block copolymer, and M. Schöps, Max-Planck Institut für Polymerforschung, Mainz, for synthesis of the homopolymer. We also thank A. Hanewald, Max-Planck Institut für Polymerforschung, Mainz, for help with the rheological measurements. Help with the analysis of the SAXS results by Dr. K. Kimishima, ERATO Polymer Phasing Project, is gratefully acknowledged. C. Graf is thanked for the synthesis of the photolabels. This work

was supported in part by the Japanese Research and Development Corp., the Emil Paul Müller Gedächtnisstiftung, and the Deutsche Forschungsgemeinschaft.

References and Notes

(1) Pusey, P. N. In *Liquids, Freezing and the Glass Transition*; Les Houches Sessions LI; Levesque, D., Hansen, J. P., Zinn-Justin, J. Eds.; Elsevier: Amsterdam, 1990; see also references therein.
(2) Hashimoto, T.; Fujimura, M.; Kawai, H. *Macromolecules* **1980**, *13*, 1660.
(3) Berney, C. V.; Cohen, R. E.; Bates, F. S. *Polymer* **1982**, *23*, 1222.
(4) Kinning, D. J.; Thomas, E. L. *Macromolecules* **1984**, *17*, 1712.
(5) Leibler, L.; Pincus, P. A. *Macromolecules* **1984**, *17*, 2922.
(6) Bywater, S. *Adv. Polym. Sci.* **1979**, *30*, 89.
(7) Halperin, A. *Macromolecules* **1987**, *20*, 2943.
(8) Bauer, B. J.; Fetters, L. J.; Graessley, W. W.; Hadjichristidis, N.; Quack, G. *Macromolecules* **1989**, *22*, 2337.
(9) Watanabe, H.; Kotaka, T.; Hashimoto, T.; Shibayama, M.; Kawai, H. *J. Rheol.* **1982**, *26*, 153.
(10) Watanabe, H.; Kotaka, T. *Polym. J.* **1983**, *15*, 337.
(11) Watanabe, H.; Kotaka, T. *Polym. Eng. Rev.* **1984**, *4*, 73.
(12) Watanabe, H.; Kotaka, T. *Macromolecules* **1983**, *16*, 769.
(13) Watanabe, H.; Kotaka, T. *Macromolecules* **1984**, *17*, 342.
(14) Watanabe, H.; Sato, T.; Osaki, K. *Macromolecules* **1996**, *29*, 113.
(15) Sato, T.; Watanabe, H.; Osaki, K.; Yao, M.-L. *Macromolecules* **1996**, *29*, 3881.
(16) Watanabe, H. *Acta Polymer* **1997**, *48*, 215.
(17) Schaertl, W.; Tsutsumi, K.; Kimishima, K.; Hashimoto, T. *Macromolecules* **1996**, *29*, 5297.
(18) Schärtl, W. *Macromol. Chem. Phys.* **1999**, *200*, 481.
(19) Watanabe, H.; Sato, T.; Osaki, K.; Hamersky, M. W.; Chapman, B. R.; Lodge, T. P. *Macromolecules* **1998**, *31*, 3740.
(20) Pfeiffer, P. *Chem. Ber.* **1915**, *48*, 1777.
(21) Pfeiffer, P. *Chem. Ber.* **1916**, *49*, 2426.
(22) Splitter, J. S.; Calvin, M. *J. Org. Chem.* **1955**, *20*, 1086.
(23) Antonietti, M.; Coutandin, J.; Gruetter, R.; Sillescu, H. *Macromolecules* **1984**, *17*, 798.
(24) Ferry, D. J. *Viscoelastic Properties of Polymers*, 3rd ed.; Wiley: New York, 1980.
(25) Matsuoka, H.; Tanaka, H.; Hashimoto, T.; Ise, N. *Phys. Rev. B* **1987**, *36*, 1754.
(26) Pakula, T.; Vlassopoulos, D.; Fytas, G.; Roovers, J. *Macromolecules* **1998**, *31*, 8931.

MA990549M